THE JOURNAL OF BIOLOGICAL CHEMISTRY VOL. 290, NO. 24, pp. 15327–15336, June 12, 2015

The Endoplasmic Reticulum Stress Sensor IRE1α in Intestinal Epithelial Cells Is Essential for Protecting against Colitis*

Received for publication, December 29, 2014, and in revised form, April 20, 2015 Published, JBC Papers in Press, April 29, 2015, DOI 10.1074/jbc.M114.633560

Hai-Sheng Zhang[‡1], Ying Chen[‡1], Li Fan[‡], Qiu-Lei Xi[§], Guo-Hao Wu[§], Xiu-Xiu Li[‡], Tang-Long Yuan[‡], Sheng-Qi He[‡], Yue Yu[‡], Meng-Le Shao[‡], Yang Liu[‡], Chen-Guang Bai[¶], Zhi-Qiang Ling[‖], Min Li[**], Yong Liu[‡2], and Jing Fang[‡§‡‡3]

*From the [‡]Laboratory of Food Safety Research, Laboratory of Nutrition and Metabolism, Institute for Nutritional Sciences, Shanghai Institutes for Biological Sciences, Chinese Academy of Sciences, Shanghai 200031, the [§]Department of Surgery, Zhongshan Hospital, Fudan University School of Medicine, Shanghai 200030, the [¶]Department of Pathology, Changhai Hospital, the Second Military Medical University, Shanghai 200433, the [‖]Department of Pathology, Zhejiang Cancer Research Institute, Zhejiang Cancer Hospital and Zhejiang Cancer Center, Hangzhou 310022, the [‡‡]Key Laboratory of Food Safety Risk Assessment, Ministry of Health, Beijing 100021, and the **Department of Surgery, University of Oklahoma Health Sciences Center, Oklahoma City, Oklahoma 73104*

Background: Endoplasmic reticulum (ER) stress is implicated in inflammatory bowel disease (IBD) and IRE1α plays a critical role in ER stress.
Results: Genetic ablation of *Ire1α* in intestinal epithelial cells leads to colitis in mice.
Conclusion: IRE1α acts as an important defense molecule against IBD.
Significance: The finding provides insight into the regulation of intestinal epithelium homeostasis by IRE1α.

Intestinal epithelial cells (IECs) have critical roles in maintaining homeostasis of intestinal epithelium. Endoplasmic reticulum (ER) stress is implicated in intestinal epithelium homeostasis and inflammatory bowel disease; however, it remains elusive whether IRE1α, a major sensor of ER stress, is directly involved in these processes. We demonstrate here that genetic ablation of *Ire1α* in IECs leads to spontaneous colitis in mice. Deletion of *IRE1α* in IECs results in loss of goblet cells and failure of intestinal epithelial barrier function. *IRE1α* deficiency induces cell apoptosis through induction of CHOP, the pro-apoptotic protein, and sensitizes cells to lipopolysaccharide, an endotoxin from bacteria. IRE1α deficiency confers upon mice higher susceptibility to chemical-induced colitis. These results suggest that IRE1α functions to maintain the intestinal epithelial homeostasis and plays an important role in defending against inflammation bowel diseases.

Inflammatory bowel disease (IBD)[4] is a chronic inflammatory condition with severe pathology (1–3), which includes two major types, Crohn's disease (CD) and ulcerative colitis (UC). The precise mechanism underlying the pathogenesis of IBD is poorly understood. A common feature of IBD is the loss of intestinal epithelial barrier function due to excessive epithelial cell death, which allows the invasion of bacteria into the submucosa, leading to inflammatory response and barrier disruption (4). The barrier relies on the turnover of intestinal epithelial cells (IECs) originating from the stem cells in the crypts. Under the physiologic state, IECs have a relatively short lifespan and their death is tightly controlled, which is critical for the maintenance of normal barrier function (5). Increased apoptosis of IECs with resultant epithelial barrier defect has a key role in the development of IBD (4, 6).

The unfolded protein response allows cells to manage endoplasmic reticulum (ER) stress resulting from accumulation of unfolded and misfolded proteins (7, 8). Three ER-localized proteins, inositol-requiring kinase/endonuclease 1 (IRE1), pancreatic ER kinase (PERK), and activating transcription factor 6 constitute the three arms of the unfolded protein response to resolve ER stress. IRE1 is the most evolutionally conserved among the three unfolded protein response arms (9, 10). In mammals, IRE1 consists of two structurally related proteins, IRE1α and IRE1β (11). IRE1 possesses both protein kinase and endoribonuclease activities. Under ER stress, IRE1α is activated through trans-autophosphorylation and dimerization/oligomerization, removing a 26-bp nucleotide intron from the mRNA encoding X-box binding protein (XBP) 1 (12). This in turn generates a spliced active form XBP1s, which regulates the expression of genes involved in protein folding, ER-associated degradation, protein quality control, and phospholipid synthesis (12). In response to ER stress, PERK is activated and phosphorylates the eukaryotic translation-initiation factor 2α (eIF2α), leading to shutdown of cellular protein translation (13). Simultaneously, the phosphorylated eIF2α stimulates the expression of C/EBP homologous protein (CHOP), a proapoptotic protein (13–16).

Many studies have shown that ER stress is linked to intestinal inflammation (11, 17–20). Genetic deletion of *Xbp1* in IECs

* This work was supported by Natural Science Foundation of China Grant 31270829, Shanghai Ministry of Science and Technology Grant 13JC1406200, Shanghai Institutes for Biological Sciences Grant 2012CSP003, the Chinese Academy of Sciences/International Partnership Program for Creative Research Teams International Partnership Program for Creative Research Teams (to J. F.), and the Ministry of Science and Technology (973 Programs 2012CB524900) and Natural Science Foundation of China Grants 31230036, 81321062, and 91213306 (to Y. L.).
[1] Both authors contributed equally to this study.
[2] To whom correspondence may be addressed. E-mail: liuy@sibs.ac.cn.
[3] To whom correspondence may be addressed. E-mail: jfang@sibs.ac.cn.
[4] The abbreviations used are: IBD, inflammatory bowel disease; IEC, intestinal epithelial cell; ER, endoplasmic reticulum; PERK, pancreatic ER kinase; IRE1, inositol-requiring kinase/endonuclease 1; XBP, X-box binding protein; DSS, dextran sulfate sodium.

caused spontaneous enteritis in mice (19), whereas deletion of *IRE1β* led to higher susceptibility to dextran sulfate sodium (DSS)-induced colitis (11). Further studies show that IRE1β optimizes the production of mucin in goblet cells, indicating that IRE1β is involved in ER homeostasis in goblet cells (21). It still remains elusive whether or not IRE1α is involved in the homeostatic control of the intestinal epithelium. In this article we report that mice in which *Ire1α* is specifically deleted in IECs develop spontaneous colitis and exhibit increased sensitivity to DSS colitis. Our results demonstrate that IRE1α acts as an important defense molecule against IBD, playing a critical role in regulating the integrity and homeostasis of intestinal epithelium.

Materials and Methods

Animals—The *Villin*-Cre transgenic mice expressing Cre recombinase specifically in intestinal epithelium (22) were obtained from the Model Animal Research Center of Nanjing University. Floxed mice ($Ire1\alpha^{flox/flox}$), in which the 121-nucleotide exon 2 of the *Ern1* (*i.e. Ire1α*) allele was flanked with two loxP recombination sites, were generated as described (23). Intestinal epithelia-specific *Ire1α* knock-out mice ($Ire1\alpha^{flox/flox}$-*Villin*-Cre) were produced by intercrossing the $Ire1\alpha^{flox/flox}$ mice with *Villin*-Cre mice. Mice were housed in laboratory cages at 23 ± 3 °C with a humidity of 35 ± 5% under a 12-h dark/light cycle. With free access to a regular chow diet (Shanghai Laboratory Animal Co. Ltd, Shanghai), animals were maintained under a specified pathogen-free condition. All protocols of animal experiments were approved by the Institutional Animal Care and Use Committee at the Institute for Nutritional Sciences.

In Vivo Intestinal Permeability Assay—Age-matched female littermates (18–20 weeks) were orally administered (0.6 mg/g body weight) a FITC-dextran solution (70 kDa, 80 mg/ml). After 4 h, the mice were sacrificed and blood was obtained by cardiac puncture. Plasma was used for FITC measurement by fluorometry (19). The distribution of FITC-dextran in colon tissues was determined by fluorescence microscopy (24).

In Vitro Permeability Assay—Caco-2 cells were cultured on Transwells with polyester membrane insert (Corning) allowing proper cellular polarization with formation of apical (upper compartment) and basolateral face (lower compartment). The insert was pretreated with DMEM overnight before cell plating. Caco-2 cells were seeded at a density of 0.5×10^5 cells/insert. The medium were replaced with fresh medium every 2 days. After 18 days, IRE1α siRNA transfection was carried out for 4 days as described (25). After transfection, the fresh medium containing FITC-dextran (10 kDa, 10 μg/ml) was added to the upper compartment and incubated at 37 °C for 4 h. The aliquots from the bottom compartment were examined for FITC-dextran in a spectrophotometer (excitation 485 nm and emission 530 nm).

Tissue Staining—Colon tissues were formalin-fixed and paraffin-embedded, and hematoxylin eosin (H&E) staining was performed. The periodic acid-Schiff (PAS) staining was performed for detection of goblet cells as described (26). Immunohistochemical staining was done as described (27).

Isolation of Colon Epithelial Cells—Colonic epithelial cells were isolated as described (11). Briefly, the colon was removed and washed with solution "A" (96 mM NaCl, 27 mM sodium citrate, 1.5 mM KCl, 0.8 mM KH_2PO_4, 5.6 mM Na_2HPO_4, 5,000 units/liter of penicillin, 5 mg/liter of streptomycin, 0.5 mM DTT, and 2 mM phenylmethylsulfonyl fluoride, pH 7.4). Square pieces of tissue were placed in 10 ml of solution A at 37 °C for 10 min with gentle shaking to remove the mucus, bacteria, and other lumenal contents. The tissue fragments were then incubated in solution "B" (0.1 mM EDTA, 115 mM NaCl, 25 mM $NaHCO_3$, 2.4 mM K_2HPO_4, 0.4 mM KH_2PO_4, 5,000 units/liters of penicillin, 5 mg/liters of streptomycin, 2.5 mM glutamine, 2 mM phenylmethylsulfonyl fluoride, and 0.5 mM DTT, pH 7.4) at 37 °C for 30 min with gentle shaking; the disruption of the mucosa and elution of cells was stopped by adjusting to 1 mM $CaCl_2$. Tissue fragments were removed, and cells recovered in the suspension were collected.

DSS-induced Colitis—The age-matched littermates (6–8 weeks) received DSS (2%) in drinking water for 9 days. Body weight was recorded daily, and rectal bleeding was assessed (0–1, normal; 2–3, blood visible; 4, gross bleeding) as described (28).

Cell Culture and Reagents—Human normal colon epithelial CCD841 cells were maintained in RPMI 1640 medium with 10% FBS, 100 units/ml of penicillin, and 100 μg/ml of streptomycin. Colon cancer Caco-2 cells were grown in DMEM with 20% FBS and the above antibiotics. Lipofectamine 2000 was from Invitrogen. Lipopolysaccharide (LPS) (*Escherichia coli* 055:B5) and FITC-dextran (70 and 10 kDa) were purchased from Sigma. DSS was from MP Biomedicals.

Immunoblotting—Immunoblotting was performed in a standard manner. The ICAM-1 and ATF4 antibodies were purchased from Santa Cruz Biotechnology. Antibodies against the cleaved caspase 3, IRE1α, eIF2α, phospho-eIF2α(Ser-51), and CHOP were products of Cell Signaling Technology. β-Actin and IRE1β antibodies were from Sigma and Abcam, respectively.

Quantitative RT-PCR—Quantitative RT-PCR was performed with β-actin as the internal control (27). The primers for mouse genes were: *Tnfα*, 5′-CCCTCACACTCAGATCATCTTCT-3′ (F), 5′-GCTACGACGTGGGCTACAG-3′ (R); *Il-1β*, 5′-GCAACTGTTCCTGAACTCAACT-3′ (F), 5′-ATCTTTTGGGGTCCGTCAACT-3′ (R); *Il-6*, 5′-TAGTCCTTCCTACCCCAATTTCC-3′ (F), 5′-TTGGTCCTTAGCCACTCCTTC-3′ (R); *Xbp1s*, 5′-GAGTCCGCAGCAGGTG-3′(F), 5′-GTGTCAGAGTCCATGGGA-3′ (R); *Xbp1u*, 5′-AAGAACACGCTTGGGAATGG-3′ (F), 5′-ACTCCCCTTGGCCTCCAC-3′ (R); *Chop*, 5′-CCTAGCTTGGCTGACAGAGG-3′ (F), 5′-CTGCTCCTTCTCCTTCATGC-3′(R); *Muc2*, 5′-CCATTCGTCACTTCATCAGC-3′ (F), 5′-GGGTGGTCTTGTGGTAGGTG-3′ (R); *β-actin*,

5′-GATCATTGCTCCTCCTGAGC-3′ (F), 5′-ACTCCTGCTTGCTGATCCAC-3′ (R). The primers for human genes were: *CHOP*, 5′-CTGGAAGCCTGGTATGAGGAT-3′ (F), 5′-CAGGGTCAAGAGTAGTGAAGGT-3′(R); *MUC-2*, 5′-TCATCGTCATCTGGGACAAG-3′ (F), 5′-GAGCGGTGGTCAAAGTTCC-3′ (R); *β-actin*, 5′-GATCATTGCTCCTCCTGAGC-3′ (F), 5′-ACTCCTGCTTGCTGATCCAC-3′ (R).

Small Interference RNA (siRNA)—siRNA oligonucleotides were purchased from Gene Pharma (Shanghai). The sense sequences are as follows: control: 5′-UUCUCCGAACGUGUCACGUTT-3′; si-IRE1α-1, 5′GCGUAAAUUCAGGACCUAU-3′; si-IRE1α-2, 5′-GGAGAGAAGCAGCAGACUU-3′; si-CHOP-1, 5′-CUGGGAAACAGCGCAUGAA-3′; si-CHOP-2, 5′-AAGAACCAGCAGAGGUCACAA-3′.

Cell Apoptosis Assay—Apoptosis of cultured cells was measured by FACS using the FITC Annexin V Apoptosis Detection Kit (BD Pharmingen). Apoptotic cells in tissues were detected by staining with a TUNEL kit (Promega).

Statistic Analysis—Statistical analysis was conducted using the unpaired two-tailed Student's *t* test or two-way analysis of variance (ANOVA) with GraphPad Prism 5.0. Data are mean ± S.E. $p < 0.05$ is considered statistically significant.

Results

IEC-specific Ablation of Ire1α Results in Spontaneous Colitis in Mice—To investigate the function of IRE1α in intestinal homeostasis, we generated mice with specific *Ire1α* deletion in IECs by intercrossing the *Ire1α*$^{flox/flox}$ mice with *Villin*-Cre mice (Fig. 1*A*). Genotyping analyses (Fig. 1*B*) indicated that *Ire1α*$^{flox/flox}$(*Ire1α*$^{+/+}$), *Ire1α*$^{flox/wt}$*Villin*-Cre (*Ire1α*$^{+/-}$), and *Ire1α*$^{flox/flox}$*Villin*-Cre (*Ire1α*$^{-/-}$) offsprings were born at a Mendelian ratio, and they developed normally. Immunoblot analysis showed that the expression of IRE1α, but not IRE1β, was efficiently abrogated from the epithelium of the small intestine and colon of *Ire1α*$^{-/-}$ mice (Fig. 1*C*). Interestingly, *Ire1α*$^{-/-}$ mice had reduced body weight (Fig. 1*D*), and the female *Ire1α*$^{-/-}$ animals showed greater weight loss (18.9%) than the males (15.8%). Visible rectal bleeding was observed in *Ire1α*$^{-/-}$ mice (Fig. 1*E*). In contrast to that in *Ire1α*$^{+/+}$ mice (0%), occurrence of visible bleeding dramatically increased in *Ire1α*$^{-/-}$ (56.1%) and *Ire1α*$^{+/-}$ (38.3%) mice (Fig. 1*F*). Of note, rectal bleeding was found more frequently in female mice (Fig. 1*F*), indicating that females had a higher susceptibility to the development of intestinal dysfunctions. Therefore, we used female mice in most of the subsequent experiments except where indicated. Deletion of IRE1α in IECs decreased colon length (Fig. 1, *G* and *H*). In addition, *Ire1α*$^{-/-}$ mice exhibited marked reductions in their survival rate (Fig. 1*I*). These results demonstrate that IRE1α deficiency in IECs causes spontaneous colitis in mice, suggesting a critical role for IRE1α in maintaining the intestinal epithelium homeostasis.

IRE1α Deficiency in IECs Impairs the Intestinal Epithelial Barrier Function—Next, we performed H&E staining of the colon tissue section and observed apparent morphological alterations, such as loss of the goblet cells, distortion, or collapse of lamina propria, as well as lymphocyte infiltration in *Ire1α*$^{-/-}$ mice relative to their *Ire1α*$^{+/+}$ littermates (Fig. 2A_1). Deletion of IRE1α had little effect on colon crypt number, but it increased the crypt length (Fig. 2A_2). Goblet cells synthesize and secrete mucins that contribute the formation of the gel-like matrix, separating the intestinal epithelium from lumen microorganisms (29). Using PAS staining to detect mucosubstances that are normally restricted to goblet cells, we found that the number of PAS-positive cells was reduced in the colon epithelium of *Ire1α*$^{-/-}$ mice (Fig. 2*B*). The mRNA expression of mucin 2 (*Muc2*) was also decreased in the colon epithelium of *Ire1α*-deficient mice (Fig. 2*C*). Because reduced goblet cells may lead to failure of epithelial barrier function, we tested this by oral FITC-dextran administration in mice. Microphotography of colon tissue sections showed more FITC-dextran that passed through the epithelial barrier in *Ire1α*$^{-/-}$ mice (Fig. 2*D*), whereas most of the dye was retained at the surface of the barrier in *Ire1α*$^{+/+}$ littermates. Consistently, *Ire1α*$^{-/-}$ mice had higher serum levels of FITC-dextran than control littermates (Fig. 2*D*). We also determined the effects of knockdown of IRE1α on paracellular permeability of the Caco-2 cell monolayer. Knockdown of IRE1α enhanced the pass of FITC-dextran through the monolayer (Fig. 2*E*). These results suggest that IRE1α deficiency results in loss of goblet cells and disrupts the epithelial barrier function of colon.

We then examined whether IRE1α deficiency in IECs altered the expression pattern of pro-inflammatory cytokines in colon mucosa. Analyses by real-time PCR showed marked elevations in the expression of *Tnfα*, *Il-1β*, and *Il-6* in colon mucosa of *Ire1α*$^{-/-}$ mice as compared with that in *Ire1α*$^{+/+}$ littermates (Fig. 2*F*). Immunostaining of the colon sections also revealed higher expression of ICAM-1, a marker of activation of immune responses (30), in *Ire1α*$^{-/-}$ mice than in *Ire1α*$^{+/+}$ littermates (Fig. 2*G*). These data indicate an exacerbated inflammatory state as a result of IRE1α deficiency in IECs.

Loss of IRE1α Promotes Cell Apoptosis in Colon Epithelium—To know how IRE1α deficiency impairs colon epithelial homeostasis, we examined *Xbp-1* mRNA splicing by real-time PCR in isolated primary colon epithelial cells. The ratio of spliced to unspliced *Xbp-1* mRNA was decreased in colon epithelial cells from *Ire1α*$^{-/-}$ mice (Fig. 3*A*). The results suggest that IRE1β cannot compensate for the absence of IRE1α in the splicing of *Xbp1* mRNA. JNK is activated by IRE1α (31). We presumed that IRE1α deletion might decrease the phosphorylation of JNK. As expected, the phosphorylation levels of JNK in colon epithelial cells of *Ire1α*$^{-/-}$ mice were reduced (Fig. 3*B*). Whereas a decreased *Xbp1* mRNA splicing and JNK phosphorylation was detected (Fig. 3, *A* and *B*), a dramatic increase of phosphorylation of eIF2α was observed (Fig. 3*C*), implying an activation of PERK signaling. The expression of CHOP, a downstream target of this signaling was also up-regulated in colon epithelial cells of *Ire1α*$^{-/-}$ mice (Fig. 3, *C* and *D*). This indicates an exacerbated state of ER stress, which may induce cell death (13–16). TUNEL stain of the colon tissue sections revealed an apparent increase in cell death in colon epithelium of *Ire1α*$^{-/-}$ mice (Fig. 3, *E* and *F*). In accord with this, increased cleavage of caspase 3 was found in colon epithelial cells of *Ire1α*$^{-/-}$ mice (Fig. 3*G*).

Next, we determined the effect of IRE1α knockdown in human normal colon epithelial CCD841 cells. siRNA-directed suppression of IRE1α expression resulted in increased eIF2α phosphorylation and up-regulated expression of CHOP (Fig. 4*A*), in parallel with increased apoptotic cells (Fig. 4*B*), suggesting that IRE1α deletion augmented the ER stress-associated death of colon epithelial cells. Similar results were obtained with Caco-2 cells (Fig. 4, *A* and *B*). The results prompt us to hypothesize that IRE1α in colon epithelium may act as a microbial sensor and defend against the detrimental effects of intes-

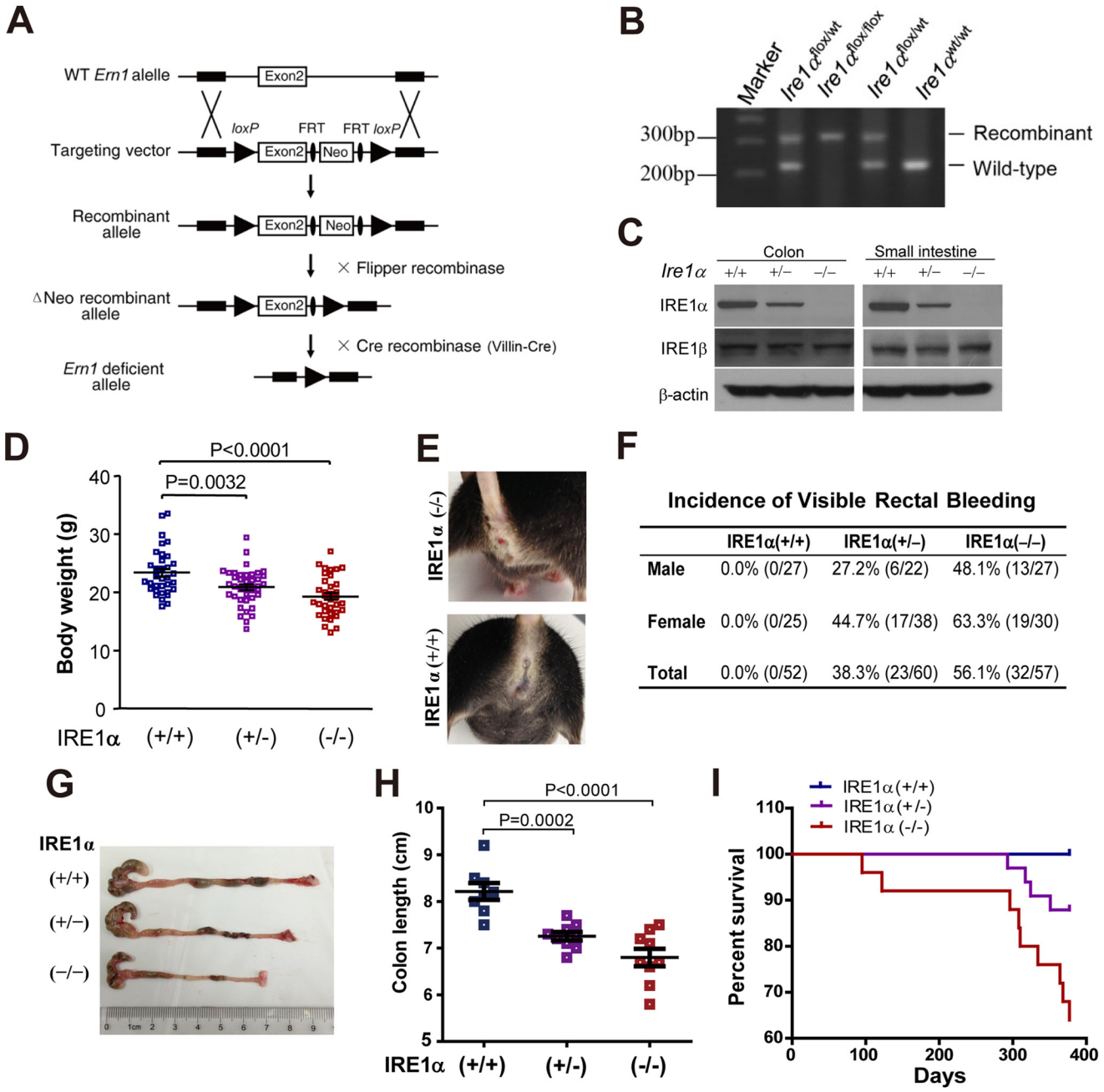

	IRE1α(+/+)	IRE1α(+/–)	IRE1α(–/–)
Male	0.0% (0/27)	27.2% (6/22)	48.1% (13/27)
Female	0.0% (0/25)	44.7% (17/38)	63.3% (19/30)
Total	0.0% (0/52)	38.3% (23/60)	56.1% (32/57)

FIGURE 1. **Mice with IEC-specific deletion of *Ire1α* develop spontaneous colitis.** *A,* schematic of the strategy for generation of the floxed mice ($Ire1\alpha^{flox/flox}$) in which the exon 2 of the *Ire1α* (*Ern1*) gene was flanked with *loxP* recombination sites as previously described in detail (23). Cre recombinase-mediated removal of the exon 2 leads to disruption of the *Ern1* allele. *Villin*-Cre mice that express the Cre recombinase transgene under the control of *Villin* promoter were used to create intestinal epithelia-specific *Ire1α* knock-out mice ($Ire1\alpha^{flox/flox}$*Villin*-Cre) by intercrossing with $Ire1\alpha^{flox/flox}$ mice. *B,* genotyping of the wild-type *Ire1α* allele, and the heterozygous and homozygous floxed-*Ire1α* allele. PCR was conducted with primers flanking the first *loxP* site, using tail genomic DNA isolated from mice. *C,* immunoblotting analysis of IRE1α protein in intestinal or colon epithelial cells isolated from age-matched (6–8 weeks) littermates of the indicated genotype. β-Actin was used as the loading control. *D,* body weight of sex- and age-matched (18–22 weeks) littermates. Data are mean ± S.E. $Ire1\alpha^{+/+}$ ($n = 31$), $Ire1\alpha^{+/-}$ ($n = 41$), $Ire1\alpha^{-/-}$ ($n = 35$). *E,* visible rectal bleeding in $Ire1\alpha^{-/-}$ mice. Shown are representative female littermates at 22 weeks of age. *F,* the incidence of visible rectal bleeding was determined in male and female mice (16–24 weeks). *G,* representative images of colons from age-matched female littermates. *H,* colon length of age-matched female littermates (18∼22 weeks). Data are mean ± S.E. $Ire1\alpha^{+/+}$ ($n = 8$), $Ire1\alpha^{+/-}$ ($n = 9$), and $Ire1\alpha^{-/-}$ ($n = 9$). *I,* survival curves. Kaplan-Meier analysis was performed. $Ire1\alpha^{+/+}$ ($n = 23$), $Ire1\alpha^{-/-}$ ($n = 25$). $p = 0.0020$ by Log-rank (Mantel-Cox) test.

tinal bacteria. LPS, an endotoxin produced by bacteria, is known to induce ER stress (32–34). It can directly cause intestinal epithelial cell apoptosis (35) and failure of intestinal barrier (36). Thus, we used CCD841 cells to determine whether IRE1α could affect the cytotoxic activity of LPS. Although LPS treatment induced cell apoptosis, knockdown of IRE1α further amplified cell apoptosis induced by LPS (Fig. 4*B*), indicating that IRE1α deficiency could sensitize CCD841 cells to LPS challenge. LPS treatment increased phosphorylation of eIF2α and expression of CHOP (Fig. 4*C*), and IRE1α knockdown together with LPS enhanced these effects (Fig. 4*D*). To further investigate the possible mechanism, we considered the involvement of CHOP, the critical molecule that has been known to mediate ER stress-induced apoptosis (13–16). Notably, knockdown by siRNAs

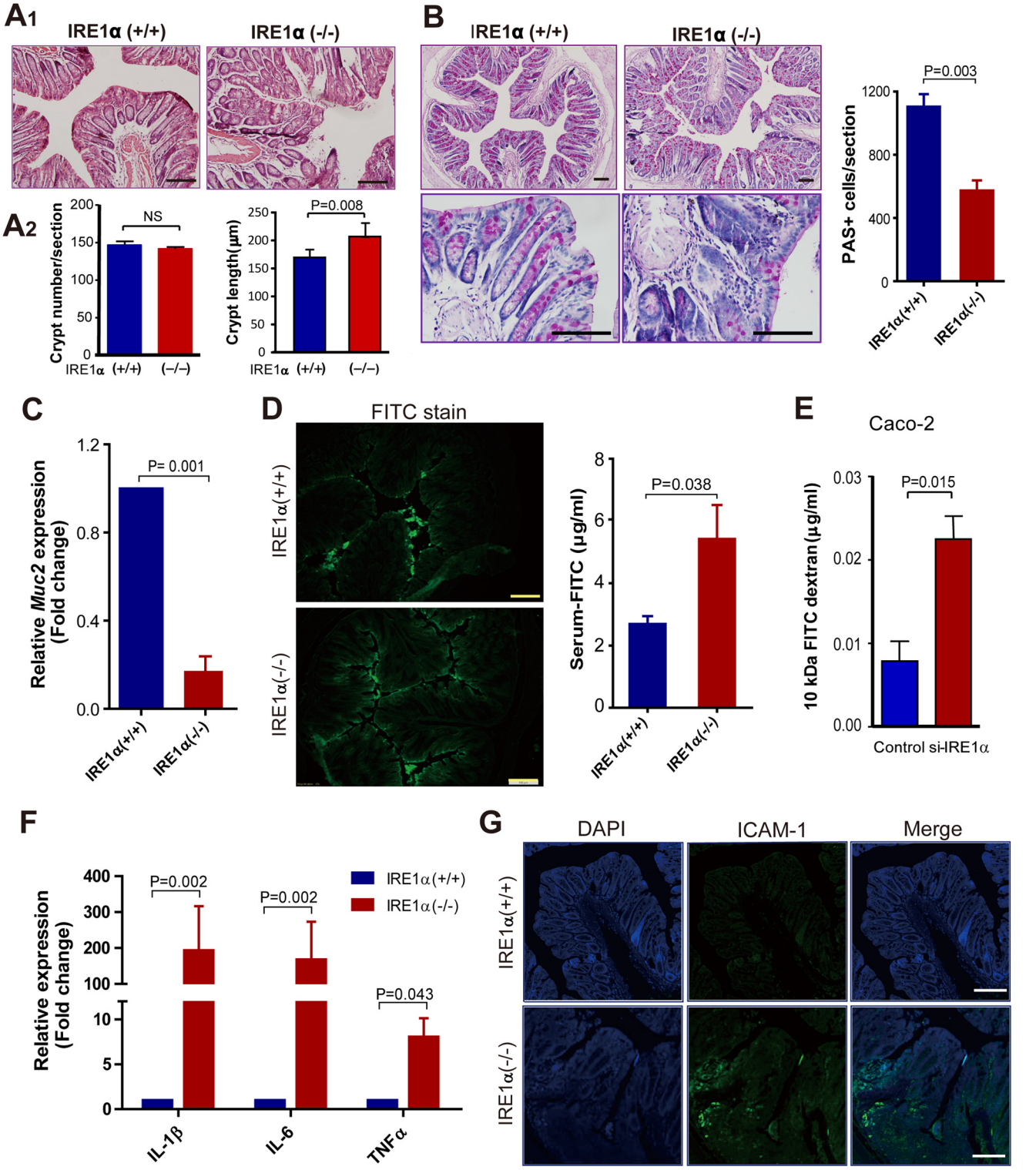

FIGURE 2. **IRE1α deficiency results in intestinal barrier dysfunction and inflammation.** *A*$_1$, H&E staining of the distal colon tissue sections of female *Ire1α*$^{+/+}$ and *Ire1α*$^{-/-}$ littermates. *A*$_2$, crypt number and length were determined. Five female mice of each genotype were examined (18–22 weeks). Crypt length was measured as described (47). *B*, PAS staining of distal colon tissue sections. PAS-positive cells were quantified using the "Image-Pro Plus" software. Data are mean ± S.E. *Ire1α*$^{+/+}$ ($n = 4$) and *Ire1α*$^{-/-}$ ($n = 6$). *C*, quantitative RT-PCR analysis of *Muc2* mRNA abundance in isolated colon epithelial cells from age-matched female mice. Values from *Ire1α*$^{+/+}$ mice were set as 1. Data are mean ± S.E. ($n = 4$). *D*, colon epithelial permeability was determined as described under "Materials and Methods." Distribution of FITC-dextran in sectioned colon tissues was analyzed by fluorescence microscopy (*left panel*). The *right panel* shows the level of FITC-dextran in serum. Data are mean ± S.E. ($n = 6$ for each phenotype). *E*, effects of knockdown of IRE1α on paracellular permeability of Caco-2 monolayer. *In vitro* paracellular permeability was performed as described under "Materials and Methods." *F*, analyses by quantitative RT-PCR of the mRNA abundance of *Tnfα*, *Il-1β*, and *Il-6* in the colon epithelium. Values from *Ire1α*$^{+/+}$ mice were set as 1. Data are mean ± S.E. *Ire1α*$^{+/+}$ ($n = 6$), *Ire1α*$^{-/-}$ ($n = 8$). *G*, staining of colon tissue sections with ICAM-1 antibody. *Scale bar* = 100 μm.

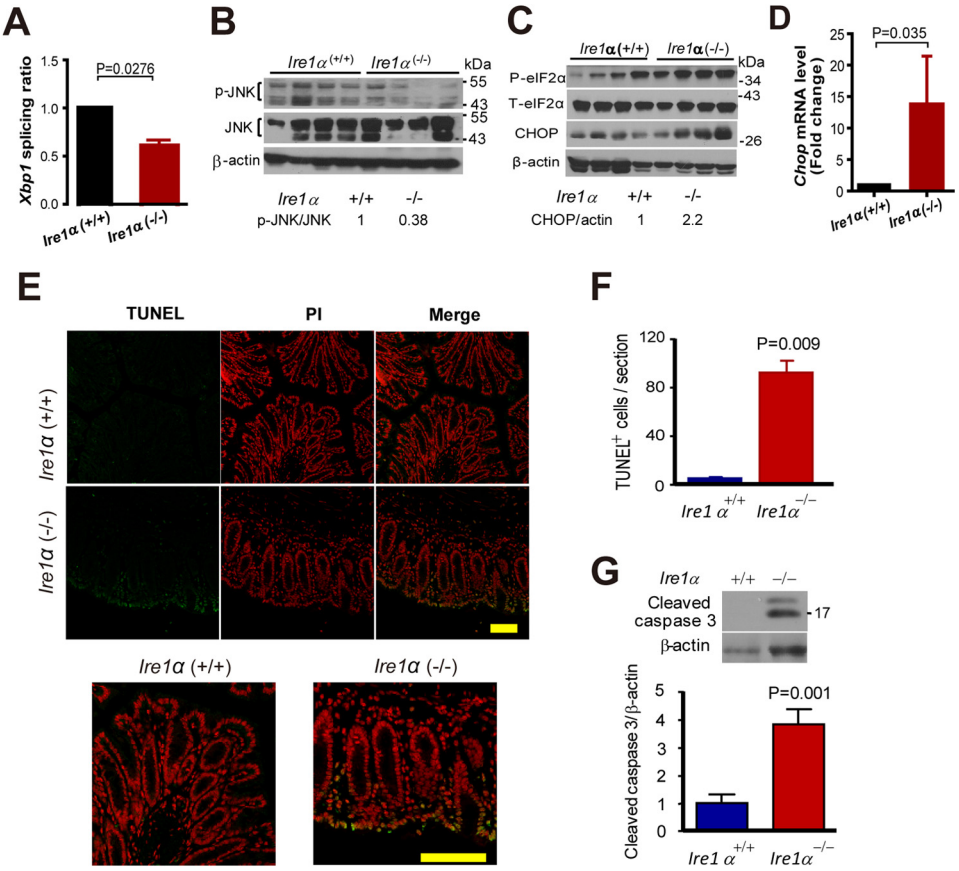

FIGURE 3. **IRE1α ablation exacerbates ER stress and apoptosis in colon epithelial cells.** *A*, analysis by real-time PCR of *Xbp1* mRNA splicing. The colon epithelial cells from age-matched female mice were isolated for the RNA preparation. The data are mean ± S.E. $Ire1^{+/+}$ ($n = 9$), $Ire1^{-/-}$ ($n = 11$). *B*, P-JNK in colon epithelial cells of $Ire1^{+/+}$ and $Ire1^{-/-}$ littermates ($n = 4$ for each phenotype). The relative *p*-JNK level was determined by measuring the density of the *p*-JNK band and normalized to that of JNK. The average *p*-JNK level of $Ire1^{+/+}$ mice is designated as 1. *C*, phosphorylation of eIF2α and expression of CHOP in colon epithelial cells of $Ire1\alpha^{-/-}$ and $Ire1\alpha^{+/+}$ mice ($n = 4$ for each phenotype). Relative CHOP level was determined as described above. *D*, quantitative RT-PCR analysis of *Chop* mRNA levels in colon epithelial cells from mice ($n = 4$). *E*, TUNEL staining of colon tissue sections from mice of the indicated genotype. The *bottom panels* are enlarged merged images. *F*, the panel shows statistic results of TUNEL-positive cells ($n = 3$). The data are mean ± S.E. *G*, increased cleavage of caspase 3 in colon epithelial cells of $Ire1\alpha^{-/-}$ mice. The *upper panel* is representative of the Western blot for cleaved caspase 3. The *lower panel* shows the relative level of cleaved caspase 3 with that of control set as 1 ($n = 5$). *Scale bar* = 100 μm.

of CHOP expression (Fig. 4*E*) blunted significantly the increases of apoptotic CCD841 cells resulting from IRE1α knockdown (Fig. 4*F*). Moreover, the repression of CHOP also abolished the IRE1α deficiency enhancement of LPS-promoted apoptosis (Fig. 4*G*). These results indicate that IRE1α can exert cytoprotective actions against toxins from bacteria, likely through managing ER stress-induced apoptosis in colon epithelia.

The above results indicate that IRE1α deletion leads to cell apoptosis (Fig. 3, *E* and *F*) and decrease of *Muc-2* mRNA (Fig. 2*C*). We determined whether the decrease of *Muc-2* mRNA is caused by cell apoptosis. We examined Caco-2 cells that produce Muc2. We found that knockdown of IRE1α induced apoptosis and decreased the *Muc2* mRNA level (Fig. 4*H*). Inhibition of cell apoptosis by caspases inhibitor Z-VAD prevented the decrease of *Muc-2* mRNA (Fig. 4*H*).

IRE1α Abrogation Confers Mice Higher Susceptibility to DSS-induced Colitis—It was documented that mice with IRE1β ablation did not develop colitis but showed increased sensitivity to DSS (11), a toxin that disrupts the barrier function and induces colitis (37). We then investigated whether IRE1α is similarly implicated in protecting cells from DSS toxicity. Upon exposure to DSS, $Ire1\alpha^{-/-}$ mice exhibited more severe wasting (Fig. 5*A*), rectal bleeding (Fig. 5*B*), and colon shortening (Fig. 5*C*) than $Ire1\alpha^{+/+}$ and $Ire1\alpha^{+/-}$ littermates. Histological analyses showed that $Ire1\alpha^{-/-}$ mice had increased crypt loss, lamina propria collapse, areas of mucosal erosions, and lymphocyte infiltration, as compared with $Ire1\alpha^{+/+}$ littermates (Fig. 5*D*). In addition, $Ire1\alpha^{-/-}$ mice showed marked decreases in goblet cells (Fig. 5*E*). The aforementioned results indicate that LPS enhanced the effects of IRE1α knockdown on cell survival *in vitro*, we next examined DSS colitis in $Ire1\alpha^{+/+}$ and $Ire1\alpha^{-/-}$ mice treated with antibiotics. Treatment with antibiotic abrogated the differences in body weight (Fig. 5*F*), colon length (Fig. 5*G*), and bleeding score (Fig. 5*H*) in DSS colitis between $Ire1\alpha^{+/+}$ and $Ire1\alpha^{-/-}$ mice, implying the importance of gut flora in the colitis observed. Moreover, $Ire1\alpha^{-/-}$ mice exhibited a slower recovery of body weight than $Ire1\alpha^{+/+}$ littermates upon removal of DSS (Fig. 5*I*). These data suggest a crucial role for IRE1α in protecting against DSS-induced colitis.

Discussion

Under ER stress, the IRE1α-XBP1 pathway plays a pivotal role in restoring ER homeostasis for cell survival. Deletion of *Xbp1* in mice IECs led to spontaneous enteritis (19). Although

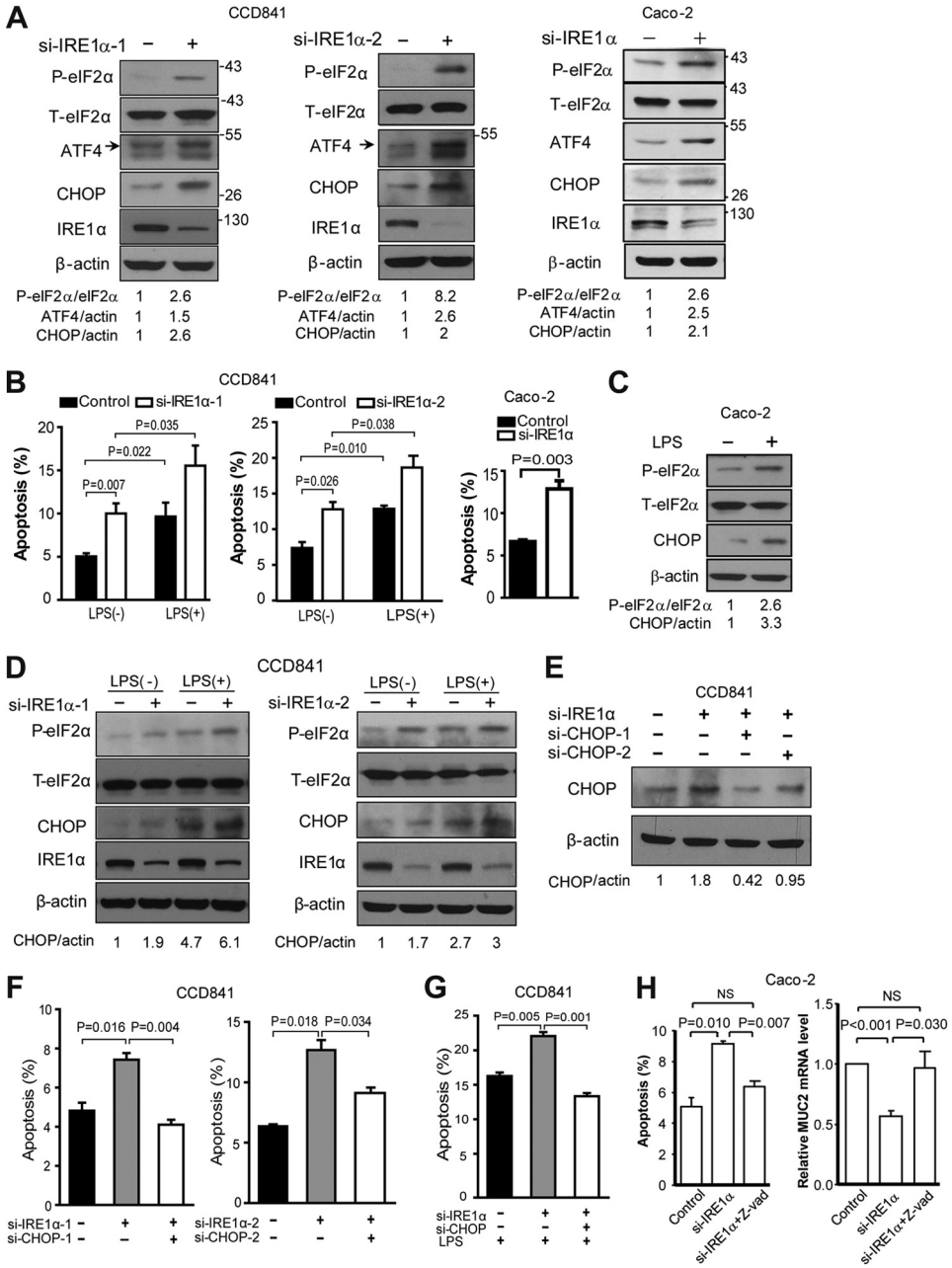

FIGURE 4. **Knockdown of IRE1α promotes LPS-induced ER stress and cell apoptosis.** *A,* CCD841 or Caco-2 cells were transfected with scrambled control siRNA or IRE1α siRNAs. After 48 h, the cells were harvested for immunoblotting. Densitometric quantification of IRE1α protein abundance is shown after normalization to β-actin, with the value of the control set as 1. *B,* CCD841 cells were transfected for 36 h with siRNAs as indicated prior to treatment with or without LPS at 2 μg/ml for 24 h. Apoptosis was measured as described under "Materials and Methods." *C,* Caco-2 cells were treated with LPS (2 μg/ml) for 24 h, followed by immunoblot analysis of eIF2α phosphorylation and CHOP expression. *D,* transfected CCD841 cells were treated with or without LPS at 2 μg/ml for 12 h, followed by immunoblot analysis of eIF2α phosphorylation and CHOP expression. *E–G,* CCD841 cells were transfected for 36 h with scrambled control siRNA, siIRE1α, and/or siCHOP as indicated. *E,* immunoblot analysis of CHOP expression in CCD841. Densitometric quantification of the CHOP protein level is shown, with the value of the siIRE1α-1 knockdown cells set as 1. *F,* cell apoptosis analysis. *G,* transfected CCD841 cells were treated with LPS at 4 μg/ml for 24 h and apoptosis was determined. *H,* Caco-2 cells were transfected with control or IRE1α siRNA oligos in the presence or absence of Z-VAD (20 μM). After 48 h, the cells were collected for determination of cell apoptosis and *Muc-2* mRNA. Data are mean ± S.E.

deletion of *Ire1β* did not result in IBD spontaneously, it sensitized mice to DSS-induced colitis (11). These promoted us to determine the possible role of IRE1α in intestinal epithelium homeostasis. We demonstrate here that IEC-specific deletion of IRE1α in mice caused spontaneous colitis and the female mice with IRE1α ablation are more susceptible to colitis. Our findings suggest that IRE1α exerts critical actions in maintaining the homeostasis of intestinal epithelium.

Our results show that deletion of IRE1α increased eIF2α phosphorylation and CHOP expression (Fig. 3), indicating the activation of the PERK pathway, another arm of unfolded protein response. Under persistent ER stress, PERK signaling induces the expression of CHOP (38), a key mediator of ER stress-associated apoptosis (14). It is well established that unresolved ER stress leads to cell apoptosis (13). The *Ire1α*$^{-/-}$ mice had more apoptotic cells in the colon epithelium, along with activated

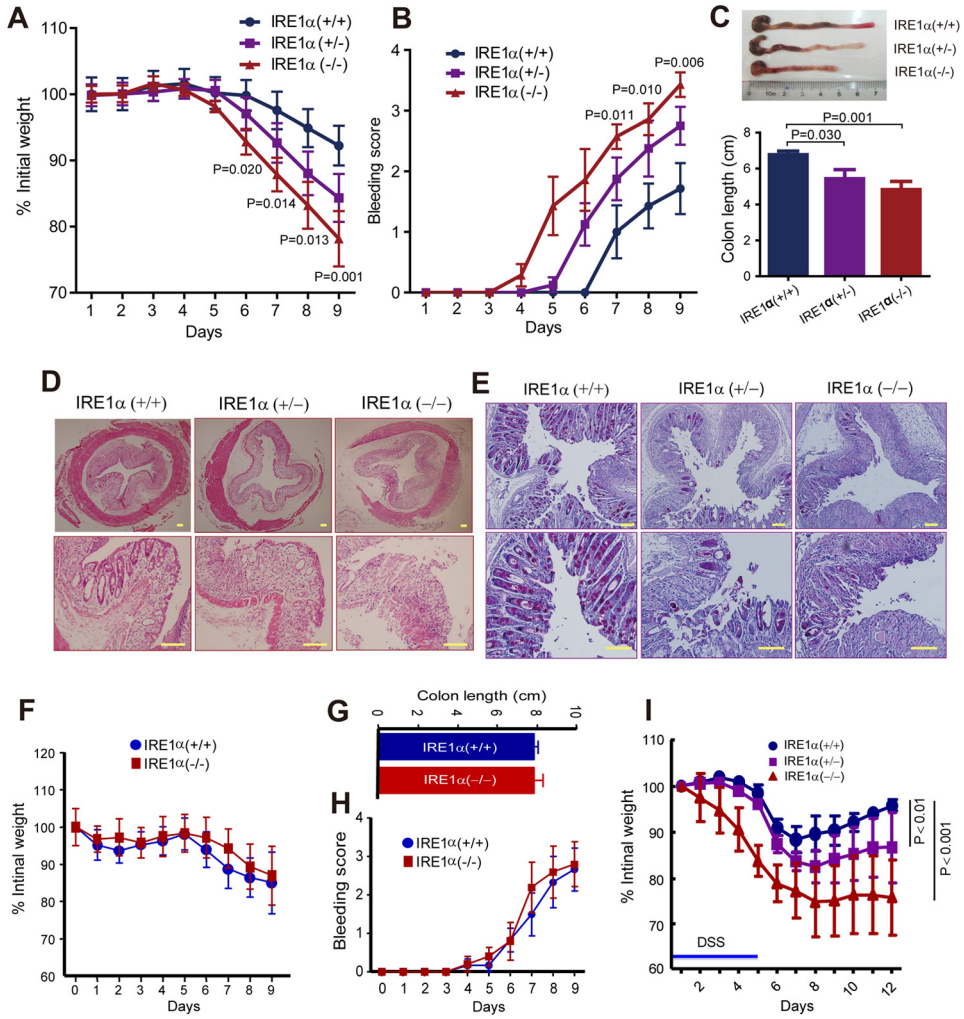

FIGURE 5. ***Ire1α*$^{-/-}$ mice are more susceptible to DSS-induced colitis.** *A–E*, age-matched (6–8 weeks) male littermates were treated with DSS (2% in drinking water) for 9 days as described under "Materials and Methods." *A,* body weight was monitored at the indicated time. Data are mean ± S.E. *Ire1α*$^{+/+}$ ($n = 9$), *Ire1α*$^{+/-}$ ($n = 11$), and *Ire1α*$^{-/-}$ ($n = 9$). *p* values are indicated for statistic analysis of *Ire1α*$^{+/+}$ *versus Ire1α*$^{-/-}$. *B,* bleeding score. Data are mean ± S.E. *p* values are indicated for statistic analysis of *Ire1α*$^{+/+}$ *versus Ire1α*$^{-/-}$. *C,* measurement of colon length. The *upper panel* shows representatives of colons and the *lower panel* shows statistic analysis of colon length. Data are mean ± S.E. *D,* H&E staining of colon tissue sections. *E,* PAS staining of colon tissue sections. *F–H,* antibiotic treatment abrogates the differences in susceptibility to DSS colitis. The experiments were performed as in *A*, except that a higher dose of DSS (3.5%) was used. Neomycin sulfate (1.5 g/liter) and metronidazole (1.5 g/liter) were added in drinking water over the examination. *F,* body weight; *G,* colon length; *H,* bleeding score. *Ire1α*$^{+/+}$ ($n = 5$), *Ire1α*$^{-/-}$ ($n = 4$). *I,* body weight recovery for mice after DSS exposure. Age-matched male mice (6–8 weeks) were exposed to 2.5% DSS for 5 days, followed by normal water ($n = 4$ per genotype). Body weight was monitored. Two-way analysis of variance was employed for statistic analysis. *Scale bar* = 100 μm.

PERK signaling (Fig. 3). Thus, cell apoptosis in IRE1α-deficient colon epithelium might result, at least in part, from the up-regulated expression of CHOP. Supporting this notion, our *in vitro* experiments showed that suppression of CHOP blunted IRE1α deficiency induced cell apoptosis (Fig. 4). These results suggest that IRE1α deficiency activates the pro-apoptotic PERK/CHOP pathway. Nonetheless, other mechanisms might also be involved, as chronic ER stress can impair cellular homeostasis through ER calcium leakage, mitochondrial damage, oxidative stress, and caspases activation (13, 39). We noted that deletion of IRE1α led to a decrease of *Xbp-1* splicing in knock-out mice (Fig. 3A). Spliced XBP-1 functions to promote cell survival. Thus, the impaired *Xbp-1* splicing may also contribute to the observed phenotypes.

Intestinal bacteria are associated with bowel inflammation (40). Host recognition of bacteria is achieved through communications between epithelial cells and microbial components such as LPS, the main bacterial product that triggers immune responses. LPS may provoke chronic inflammation to damage colon epithelial cells, leading to failure of barrier function. We found that LPS activated eIF2α and induced CHOP (Fig. 4). The underlying mechanism is not clear, which needs further study. Our results show that loss of IRE1α rendered cells more susceptible to LPS challenge, and repression of CHOP could dampen the IRE1α deficiency amplified LPS induction of apoptosis of colon epithelial cells (Fig. 4). Thus, IRE1α may act to protect intestinal epithelial cells from LPS-elicited damage, contributing to the intestinal epithelial homeostasis and barrier function. Deletion of IRE1α led to increased inflammatory factors including TNFα that may also contribute to increased apoptosis of the intestinal epithelial cells.

Goblet cells are critical in epithelial defense against luminal stimulants and pathogens (41, 42). They produce and secrete mucins to lubricate and cover the intestinal epithelium. Loss of

goblet cells could be one of the causes of barrier dysfunction. In human IBD and animal colitis, disease progression is associated with the depletion of goblet cells (43, 44). We show here that deletion of IRE1α resulted in reduction of goblet cells (Fig. 2). This might be, at least in part, attributable to the exacerbated ER stress caused by IRE1α deficiency.

IBD is known to occur in genetically susceptible individuals under certain influences of environmental factors (45). ER stress is linked to the pathogenic progression of IBD (46). Single-nucleotide polymorphisms within the *XBP1* gene have been shown to confer a higher risk for IBD in the human population (19). Similarly, studies of potential genetic association of *IRE1α* with IBD will provide valuable insights into the role of ER stress in the pathogenic progression of this disease.

Our results show that genetic ablation of *Ire1α* in IECs activates PERK signaling and leads to colitis in mice, which supports the consensus that ER stress is linked to intestinal inflammation. IECs are emerging as critical mediators of inflammatory and immune responses in mucosal tissues. Our findings demonstrate that *IRE1α* is essential for epithelial protection, suggesting that it may serve as a key regulator of intestinal epithelium homeostasis. IRE1α loss in IECs causes persistent and excessive ER stress that can trigger inflammation and disrupts intestinal epithelial functions. Further elucidation of the mechanisms by which IRE1α protects the intestinal epithelial integrity and homeostasis may open avenues for new therapeutic strategies against IBD.

References

1. Baumgart, D. C., and Carding, S. R. (2007) Inflammatory bowel disease: cause and immunobiology. *Lancet* **369,** 1627–1640
2. Braus, N. A., and Elliott, D. E. (2009) Advances in the pathogenesis and treatment of IBD. *Clin. Immunol.* **132,** 1–9
3. Rutgeerts, P., Vermeire, S., and Van Assche, G. (2009) Biological therapies for inflammatory bowel diseases. *Gastroenterology* **136,** 1182–1197
4. Abraham, C., and Cho, J. H. (2009) Inflammatory bowel disease. *N. Engl. J. Med.* **361,** 2066–2078
5. Hall, P. A., Coates, P. J., Ansari, B., and Hopwood, D. (1994) Regulation of cell number in the mammalian gastrointestinal tract: the importance of apoptosis. *J. Cell Sci.* **107,** 3569–3577
6. Schulzke, J. D., Ploeger, S., Amasheh, M., Fromm, A., Zeissig, S., Troeger, H., Richter, J., Bojarski, C., Schumann, M., and Fromm, M. (2009) Epithelial tight junctions in intestinal inflammation. *Ann. N.Y. Acad. Sci.* **1165,** 294–300
7. Ron, D., and Walter, P. (2007) Signal integration in the endoplasmic reticulum unfolded protein response. *Nat. Rev. Mol. Cell Biol.* **8,** 519–529
8. Todd, D. J., Lee, A.-H., and Glimcher, L. H. (2008) The endoplasmic reticulum stress response in immunity and autoimmunity. *Nat. Rev. Immunol.* **8,** 663–674
9. Cox, J. S., Shamu, C. E., and Walter, P. (1993) Transcriptional induction of genes encoding endoplasmic reticulum resident proteins requires a transmembrane protein kinase. *Cell* **73,** 1197–1206
10. Mori, K., Ma, W., Gething, M.-J., and Sambrook, J. (1993) A transmembrane protein with a cdc2+CDC28-related kinase activity is required for signaling from the ER to the nucleus. *Cell* **74,** 743–756
11. Bertolotti, A., Wang, X., Novoa, I., Jungreis, R., Schlessinger, K., Cho, J. H., West, A. B., and Ron, D. (2001) Increased sensitivity to dextran sodium sulfate colitis in IRE1β-deficient mice. *J. Clin. Investig.* **107,** 585–593
12. Hetz, C. (2012) The unfolded protein response: controlling cell fate decisions under ER stress and beyond. *Nat. Rev. Mol. Cell Biol.* **13,** 89–102
13. Sano, R., and Reed, J. C. (2013) ER stress-induced cell death mechanisms. *Biochim. Biophys. Acta* **1833,** 3460–3470
14. Oyadomari, S., and Mori, M. (2004) Roles of CHOP//GADD153 in endoplasmic reticulum stress. *Cell Death Differ.* **11,** 381–389
15. Shore, G. C., Papa, F. R., and Oakes, S. A. (2011) Signaling cell death from the endoplasmic reticulum stress response. *Curr. Opin. Cell Biol.* **23,** 143–149
16. Tabas, I., and Ron, D. (2011) Integrating the mechanisms of apoptosis induced by endoplasmic reticulum stress. *Nat. Cell Biol.* **13,** 184–190
17. Eri, R. D., Adams, R. J., Tran, T. V., Tong, H., Das, I., Roche, D. K., Oancea, I., Png, C. W., Jeffery, P. L., Radford-Smith, G. L., Cook, M. C., Florin, T. H., and McGuckin, M. A. (2011) An intestinal epithelial defect conferring ER stress results in inflammation involving both innate and adaptive immunity. *Mucosal Immunol.* **4,** 354–364
18. Heazlewood, C. K., Cook, M. C., Eri, R., Price, G. R., Tauro, S. B., Taupin, D., Thornton, D. J., Png, C. W., Crockford, T. L., Cornall, R. J., Adams, R., Kato, M., Nelms, K. A., Hong, N. A., Florin, T. H., Goodnow, C. C., and McGuckin, M. A. (2008) Aberrant mucin assembly in mice causes endoplasmic reticulum stress and spontaneous inflammation resembling ulcerative colitis. *PLoS Med.* **5,** e54
19. Kaser, A., Lee, A.-H., Franke, A., Glickman, J. N., Zeissig, S., Tilg, H., Nieuwenhuis, E. E., Higgins, D. E., Schreiber, S., Glimcher, L. H., and Blumberg, R. S. (2008) XBP1 links ER stress to intestinal inflammation and confers genetic risk for human inflammatory bowel disease. *Cell* **134,** 743–756
20. Shkoda, A., Ruiz, P. A., Daniel, H., Kim, S. C., Rogler, G., Sartor, R. B., and Haller, D. (2007) Interleukin-10 blocked endoplasmic reticulum stress in intestinal epithelial cells: impact on chronic inflammation. *Gastroenterology* **132,** 190–207
21. Tsuru, A., Fujimoto, N., Takahashi, S., Saito, M., Nakamura, D., Iwano, M., Iwawaki, T., Kadokura, H., Ron, D., and Kohno, K. (2013) Negative feedback by IRE1β optimizes mucin production in goblet cells. *Proc. Natl. Acad. Sci. U.S.A.* **110,** 2864–2869
22. el Marjou, F., Janssen, K.-P., Chang, B. H., Li, M., Hindie, V., Chan, L., Louvard, D., Chambon, P., Metzger, D., and Robine, S. (2004) Tissue-specific and inducible Cre-mediated recombination in the gut epithelium. *genesis* **39,** 186–193
23. Shao, M., Shan, B., Liu, Y., Deng, Y., Yan, C., Wu, Y., Mao, T., Qiu, Y., Zhou, Y., Jiang, S., Jia, W., Li, J., Li, J., Rui, L., Yang, L., and Liu, Y. (2014) Hepatic IRE1α regulates fasting-induced metabolic adaptive programs through the XBP1s: PPARα axis signalling. *Nat. Commun.* **5,** 3528
24. Tambuwala, M. M., Cummins, E. P., Lenihan, C. R., Kiss, J., Stauch, M., Scholz, C. C., Fraisl, P., Lasitschka, F., Mollenhauer, M., Saunders, S. P., Maxwell, P. H., Carmeliet, P., Fallon, P. G., Schneider, M., and Taylor, C. T. (2010) Loss of prolyl hydroxylase-1 protects against colitis through reduced epithelial cell apoptosis and increased barrier function. *Gastroenterology* **139,** 2093–2101
25. Al-Sadi, R., Khatib, K., Guo, S., Ye, D., Youssef, M., and Ma, T. (2011) Occludin regulates macromolecule flux across the intestinal epithelial tight junction barrier. *Am. J. Physiol. Gastrointest. Liver Physiol.* **300,** G1054–1064
26. van Es, J. H., de Geest, N., van de Born, M., Clevers, H., and Hassan, B. A. (2010) Intestinal stem cells lacking the Math1 tumour suppressor are refractory to Notch inhibitors. *Nat. Commun.* **1,** 18
27. Xue, J., Li, X., Jiao, S., Wei, Y., Wu, G., and Fang, J. (2010) Prolyl hydroxylase-3 is down-regulated in colorectal cancer cells and inhibits IKKβ independent of hydroxylase activity. *Gastroenterology* **138,** 606–615
28. Cummins, E. P., Seeballuck, F., Keely, S. J., Mangan, N. E., Callanan, J. J., Fallon, P. G., and Taylor, C. T. (2008) The hydroxylase inhibitor dimethyloxalylglycine is protective in a murine model of colitis. *Gastroenterology* **134,** 156–165.e151
29. Specian, R. D., and Oliver, M. G. (1991) Functional biology of intestinal goblet cells. *Am. J. Physiol.* **260,** C183–C193
30. Seth, R., Raymond, F. D., and Makgoba, M. W. (1991) Circulating ICAM-1 isoforms: diagnostic prospects for inflammatory and immune disorders. *Lancet* **338,** 83–84
31. Urano, F., Wang, X., Bertolotti, A., Zhang, Y., Chung, P., Harding, H. P., and Ron, D. (2000) Coupling of stress in the ER to activation of JNK protein kinases by transmembrane protein kinase IRE1. *Science* **287,** 664–666
32. Alhusaini, S., McGee, K., Schisano, B., Harte, A., McTernan, P., Kumar, S.,

and Tripathi, G. (2010) Lipopolysaccharide, high glucose and saturated fatty acids induce endoplasmic reticulum stress in cultured primary human adipocytes: salicylate alleviates this stress. *Biochem. Biophys. Res. Commun.* **397,** 472–478
33. Dong, M., Hu, N., Hua, Y., Xu, X., Kandadi, M. R., Guo, R., Jiang, S., Nair, S., Hu, D., and Ren, J. (2013) Chronic Akt activation attenuated lipopolysaccharide-induced cardiac dysfunction via Akt/GSK3β-dependent inhibition of apoptosis and ER stress. *Biochim. Biophys. Acta* **1832,** 848–863
34. Endo, M., Mori, M., Akira, S., and Gotoh, T. (2006) C/EBP Homologous Protein (CHOP) Is crucial for the induction of caspase-11 and the pathogenesis of lipopolysaccharide-induced inflammation. *J. Immunol.* **176,** 6245–6253
35. Jarry, A., Bossard, C., Bou-Hanna, C., Masson, D., Espaze, E., Denis, M. G., and Laboisse, C. L. (2008) Mucosal IL-10 and TGF-β play crucial roles in preventing LPS-driven, IFN-γ–mediated epithelial damage in human colon explants. *J. Clin. Investig.* **118,** 1132–1142
36. Yue, C., Wang, W., Tian, W. L., Huang, Q., Zhao, R. S., Zhao, Y. Z., Li, Q. R., and Li, J. S. (2013) Lipopolysaccharide-induced failure of the gut barrier is site-specific and inhibitable by growth hormone. *Inflamm. Res.* **62,** 407–415
37. Strober, W., Fuss, I. J., and Blumberg, R. S. (2002) The immunology of mucosal models of inflammation. *Annu. Rev. Immunol.* **20,** 495–549
38. Lin, J. H., Li, H., Yasumura, D., Cohen, H. R., Zhang, C., Panning, B., Shokat, K. M., Lavail, M. M., and Walter, P. (2007) IRE1 signaling affects cell fate during the unfolded protein response. *Science* **318,** 944–949
39. Malhotra, J. D., Miao, H., Zhang, K., Wolfson, A., Pennathur, S., Pipe, S. W., and Kaufman, R. J. (2008) Antioxidants reduce endoplasmic reticulum stress and improve protein secretion. *Proc. Natl. Acad. Sci. U.S.A.* **105,** 18525–18530
40. Abraham, C., and Medzhitov, R. (2011) Interactions between the host innate immune system and microbes in inflammatory bowel disease. *Gastroenterology* **140,** 1729–1737
41. Itoh, H., Beck, P. L., Inoue, N., Xavier, R., and Podolsky, D. K. (1999) A paradoxical reduction in susceptibility to colonic injury upon targeted transgenic ablation of goblet cells. *J. Clin. Investig.* **104,** 1539–1547
42. Laukoetter, M. G., Nava, P., and Nusrat, A. (2008)) Role of the intestinal barrier in inflammatory bowel disease. *World J. Gastroenterol.* **14,** 401–407
43. Strugala, V., Dettmar, P. W., and Pearson, J. P. (2008) Thickness and continuity of the adherent colonic mucus barrier in active and quiescent ulcerative colitis and Crohn's disease. *Int. J. Clin. Pract.* **62,** 762–769
44. Van der Sluis, M., De Koning, B. A., De Bruijn, A. C., Velcich, A., Meijerink, J. P., Van Goudoever, J. B., Büller, H. A., Dekker, J., Van Seuningen, I., Renes, I. B., and Einerhand, A. W. (2006) Muc2-deficient mice spontaneously develop colitis, indicating that MUC2 is critical for colonic protection. *Gastroenterology* **131,** 117–129
45. Colgan, S. P., Curtis, V. F., and Campbell, E. L. (2013) The inflammatory tissue microenvironment in IBD. *Inflamm. Bowel Dis.* **19,** 2238–2244
46. Kaser, A., and Blumberg, R. S. (2009) Endoplasmic reticulum stress in the intestinal epithelium and inflammatory bowel disease. *Semin. Immunol.* **21,** 156–163
47. Rose, W. A., 2nd, Sakamoto, K., and Leifer, C. A. (2012) TLR9 is important for protection against intestinal damage and for intestinal repair. *Sci. Rep.* **2,** 574